To cite this article: CHEN L Y, XIE X. Bandgap optimization for chiral acoustic metamaterials based on material selection method [J/OL]. Chinese Journal of Ship Research, 2023, 18(2). http://www.ship-research.com/en/article/doi/10.19693/j.issn.1673-3185.03078.

DOI: 10.19693/j.issn.1673-3185.03078

Bandgap optimization for chiral acoustic metamaterials based on material selection method

CHEN Luyun[*1], *XIE Xing*[2]

1 State Key Laboratory of Ocean Engineering, Shanghai Jiao Tong University, Shanghai 200240, China

2 Wuhan Second Ship Design and Research Institute, Wuhan 430205, China

Abstract: [**Objectives**] The purpose of this paper is to expand the bandgap frequency of acoustic metamaterial and reduce the lower bound frequency by analysis and optimizing the bandgap parameters. [**Methods**] The influence of geometrical and material parameters on the bandgap properties of acoustic metamaterials is analyzed, and a method for maximizing the bandgap width is proposed. The multi-objective optimization problem is converted into a single objective optimization problem by normalizing the bandgap frequency coefficients. Structural material conversion is achieved via the material selection optimization method, and the optimization function of bandgap parameters are established on the basis of weight-lightening. For chiral acoustic metamaterials, the material properties (density and wave velocity) and geometric parameters (scatterer diameter, ligament thickness and coating thickness) are defined as design variables, and the comprehensive optimization of structural parameters and material selection of acoustic metamaterials based on weight-lightening are implemented. [**Results**] The optimization results show that the bandgap width increases by 27.7% and the lower bound frequency decreases by 1 048 Hz, the goal of expanding the bandgap width based on lightweight acoustic metamaterials are obtained. The acoustic transmission analysis of the finite chiral acoustic metamaterial structure is carried out to verify the effectiveness of the proposed method. [**Conclusions**] The results show that the goal of lightweight acoustic metamaterials can be effectively achieved by integrating the comprehensive optimization of structural parameters and materials. The study provides more understanding the design and application of innovative acoustic metamaterial.

Key words: acoustic metamaterials; material selection; bandgaps optimization; normalizing; acoustic transmission

CLC number: U668.5; TB34

0 Introduction

Various new functional materials have been widely used to aim the development of science and technology [1]. Particularly, acoustic metamaterials with periodically varying internal elastic constants and density induced by their specially designed microstructures can be used to suppress and control acoustic/elastic waves [2-3]. The special acoustic properties of acoustic metamaterials mainly derive from their topological structures, the negative equivalent mass density, negative equivalent bulk modulus, or negative shear modulus of such metamaterials can be attributed [4-5].

Among acoustic metamaterials, periodically arranged macroscopic medium materials will hinder the propagation of acoustic/elastic waves in the manner of scattering and phase cancellation of incident acoustic/elastic waves at particular frequencies. Such frequency intervals featuring the suppression of acoustic/elastic waves are called bandgaps [6-7]. Reducing the lower bound frequency

Received: 2022－09－10 **Accepted**: 2022－12－31

Supported by: High-tech ship research program (Lianzhuanghan [2016] No. 548)

Authors: CHEN Luyun, male, born in 1975, Ph.D., associate professor. Research interest: new materials for structural vibration and noise reduction. E-mail: cluyun@sjtu.edu.cn

XIE Xing, male, born in 1994, Ph.D., engineer. Research interest: structural design and research of ships. E-mail: 824506862@qq.com

***Corresponding author**: CHEN Luyun

downloaded from www.ship-research.com

of bandgaps and expanding bandgap widths to effectively meet the needs of vibration and noise reduction in the middle- and low-frequency bands have become a hot research issue for acoustic metamaterials [8-9]. Ligament-based chiral structures are typical structures with negative Poisson's ratios. Such structures can be divided into hexa-chiral, tetra-chiral, and tri-chiral structures, as well as corresponding anti-chiral structures, according to the number of ligaments [10]. The centerlines of the six ligaments in the commonly used hexa-chiral acoustic metamaterials are distributed at equal angles and are tangent to cylindrical scatterers. These characteristics of chiral acoustic metamaterials increase the number of variables in structural design and can thus facilitate the regulation of bandgap parameters. In addition, the resonating units in chiral structures enable the easy attainment of double-negative characteristics [11-13].

The bandgap widths and positions of acoustic metamaterials depend on the interactions among the scatterers inside these metamaterials and elastic waves. Factors affecting bandgaps mainly include structural parameters (geometry, filling rate, lattice form), material parameters (density ratio, modulus ratio, Poisson ratio, wave velocity, anisotropy), multiphase material distribution, and interface parameters [14-15]. Bandgap parameters can be adjusted or controlled by optimizing the micro-structured cell, which can improve the effects of vibration and noise reduction, especially in the low-frequency band [16-18]. However, the scatterer involved in most studies at present are made of high density metallic materials, and it give an important influence on the structural mass, and ultimately restrict their engineering applications. At present, most studies focus on optimizing the shape or topology of the scatterers in acoustic metamaterials, and lightweight design problems such as excessive mass or material consumption are often ignored. Therefore, bandgap characteristics need to be optimized on the basis of lightweighting acoustic metamaterials, and it is of important theoretical value and engineering significance for enhancing the bandgap properties of acoustic metamaterials.

Focusing on hexa-chiral acoustic metamaterials, the goal to reduce the lower-bound frequencies and expanding the widths of bandgaps is defined. Specifically, they applied an optimization algorithm to implement design parameter optimization and material selection for the cells of such acoustic metamaterials, thereby improving the bandgap properties of the acoustic metamaterials, especially in low-frequency bands.

1 Hexa-chiral acoustic metamaterials

1.1 Overview of acoustic metamaterials

A hexa-chiral acoustic metamaterial has an orthohexagonal lattice structure. The unit cell contains a cylindrical nodal ring and six uniformly distributed ligaments that are externally tangent to the ring. Each ligament is connected to another nodal ring and tangent to that ring. This repeats to complete the whole structure. In the cell structure, the distance between two cylindrical nodal rings (namely, the lattice constant) is a; the length of is L and with thickness of t_b; the inner radius of the nodal ring is r_0 with thickness of t_c. Fig. 1 shows the cell structure of a hexa-chiral acoustic metamaterial. Specifically, Fig. 1(a) shows the two-dimensional structure of the hexa-chiral acoustic metamaterial, in which $\boldsymbol{e}_1$ and $\boldsymbol{e}_2$ are position vectors of the two-dimensional cell structure. Fig. 1(b) shows the cell structure of the acoustic metamaterial. The shaded zone in Fig. 1(c) is the reduced Brillouin zone of the acoustic metamaterial. Three high-symmetry points are $\Gamma(0,0)$, $\mathrm{M}(0,\frac{2\sqrt{3}}{3})\frac{\pi}{a}$ and $\mathrm{K}(\frac{2}{3},\frac{2\sqrt{3}}{3})\frac{\pi}{a}$, respectively, the shaded part is the irreducible Brillouin zone.

1.2 Cell mass of acoustic metamaterials

In the acoustic metamaterial, as shown in Fig. 1, the mass G_{total} of a unit cell structure can be given by

$$G_{\text{total}} = G_{\text{w}} + G_{\text{r}} + G_{\text{b}} + G_{\text{s}} \tag{1}$$

where $G_{\text{w}} = S_{\text{w}}\rho_{\text{w}}$ is the mass of the matrix, S_{w} is the cross-section area of the matrix and ρ_{w} is the material density of the matrix; $G_{\text{r}} = S_{\text{r}}\rho_{\text{r}}$ is the mass of a ligament, S_{r} is the cross-section area of the ligament and ρ_{r} is the material density of the ligament; $G_{\text{b}} = S_{\text{b}}\rho_{\text{b}}$ is the mass of the coating, with S_{b} is the cross-sectional area of the coating and ρ_{b} is the material density of the coating; $G_{\text{s}} = S_{\text{s}}\rho_{\text{s}}$ is the mass of the scatterer, S_{s} is the cross-section area of the scatterer and ρ_{s} is the material density of the scatterer. It is assumed that the coating and the ligaments are made by the same material. Only the mass of the scatterer, the ligaments, and the coating be considered to simplify the calculation. In the

downloaded from www.ship-research.com

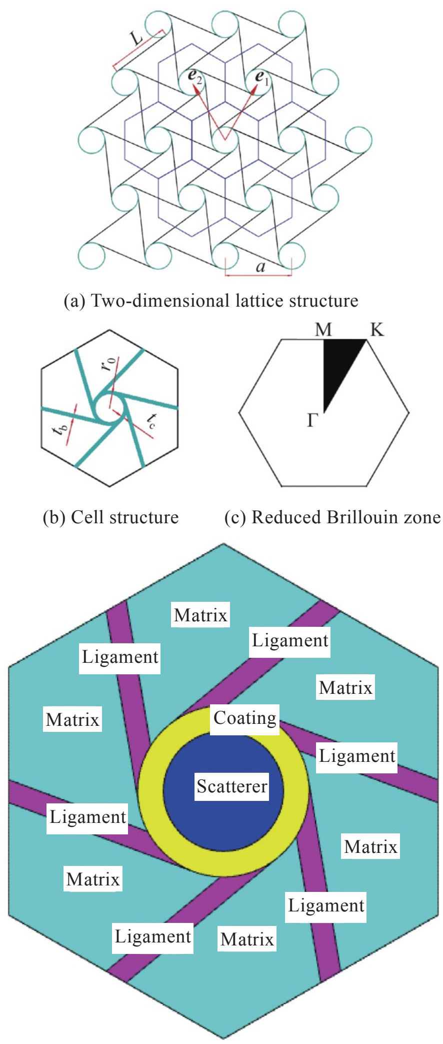

(a) Two-dimensional lattice structure

(b) Cell structure (c) Reduced Brillouin zone

(d) Components of cell structure

Fig. 1 Hexa-chiral acoustic metamaterials and Brillouin zones

lightweight design, the cell mass G_{total} was defined as a constraint and guaranteed that the total mass was not increased after optimization.

2 Bandgap optimization function for two-dimensional acoustic metamaterial

2.1 Bandgap parameters

The irreducible Brillouin zone in the acoustic metamaterial was swept by wave vector $\boldsymbol{k}$. The wave vector $\boldsymbol{k}$ be defined as horizontal coordinates, the eigenvalue or its corresponding parameter (such as frequencies) be defined as longitudinal coordinates, then the band structure or linear dispersion relationship can be drawn. The band structure had p bands and q bandgaps within the determined frequency range. If the first complete bandgap is located between the n-th and (n+1)-th bands, then the complete bandgap width can then be written as:

$$\begin{cases}\Delta\omega_n = \min[\omega_{n+1}(k)] - \max[\omega_n(k)] \\ \omega_{\mathrm{c}} = \{\min[\omega_{n+1}(k)] + \max[\omega_n(k)]\}/2\end{cases} \tag{2}$$

where $\max[\omega_n(k)]$ is the maximum frequency of the lower bound frequency; $\min[\omega_{n+1}(k)]$ is the minimum frequency of the upper-bound band corresponding to the bandgap, satisfying $\min[\omega_{n+1}(k)] > \max[\omega_n(k)]$. In present work, the width and lower bound frequency of the first complete bandgap are discussed.

2.2 Bandgap parameter coefficients

The design parameters and material parameter of the acoustic metamaterial can be optimized the bandgap width $\Delta\omega_n$ and lower bound frequency $\max[\omega_n(k)]$ of the bandgap. To obtain a larger bandgap width and a smaller lower bound frequency, it is a multiobjective optimization problem which involves two types of parameters, namely, the bandgap width and the lower bound frequency. The multiobjective problem needed to be normalized in the optimization the bandgap parameters of the acoustic metamaterial. Coefficient ξ is defined to describe the influence factor on complete bandgap width, and coefficient ς is defined to describe the influence factor on the lower bound frequency, the normalizing coefficient can be written as.

$$\begin{cases}\varsigma = \dfrac{[\max:\omega_n(k)]_0}{[\max:\omega_n(k)]^*} \\ \xi = \dfrac{(\Delta\omega_n)^*}{(\Delta\omega_n)_0}\end{cases} \tag{3}$$

where $[\max:\omega_n(k)]_0$ and $[\max:\omega_n(k)]^*$ are the lower bound frequency of the bandgap of initial design and optimized design, respectively; $(\Delta\omega_n)_0$ and $(\Delta\omega_n)^*$ are the bandgap widths of initial design and optimized design, respectively. By normalized the complete bandgap width coefficient ξ and the lower bound frequency coefficient ς, the normalization value ψ can be expressed as

$$\psi = w \cdot \xi + (1 - w) \cdot \varsigma \tag{4}$$

where w is the weight coefficient of the objective function and it satisfied to the constraint $w \in [0, 1]$. The weight coefficients depend on the goal of bandgap optimization, i.e., w = 1 means that only the complete bandgap width parameter is considered in the objective function, and w = 0 means that only the lower bound frequency parameter is considered. If the designers pay more attention on the complete bandgap width parameter, the weight coefficients for the bandgap width parameter increase, and vice versa. According to Eq. (4), the multiobjective optimization problem is converted into a single objective optimization problem. In the present work,

downloaded from www.ship-research.com

w = 0.5 is defined.

2.3 Concept of material selection

Scatterer, ligament, and coating materials are selected in the lightweight design of the cell structure. This is a distribution optimizing problem with different materials in the design domain, it is essentially an topological optimization of material distribution. The distribution of various materials in structural design domain are optimized by the conversion among different materials. This is a discrete-variable problem problem in which the elastic modulus of the material defining as the design variable.

The elastic modulus (shear modulus) of the acoustic metamaterial is an important index to evaluate the mechanical parameters of the material. The mechanical parameters, such as density, acoustic velocity, and Poisson's ratio, the given material can be considered. If the elastic modulus parameters is defined, then the othere parameter is defined are determined . The elastic modulus of the metal material of the scatterer was defined as E_s, and the non-metal material of the ligaments and coating were defined as E_r.

According to the material selection theory, the elastic model of scatterer materials can be written as $\boldsymbol{E}_s \in \{\boldsymbol{E}_{s,1}, \boldsymbol{E}_{s,2}, \ldots, \boldsymbol{E}_{s,j}\}$ (where j is the number of selected metal types). Moreover, the elastic model of the ligaments and the coating can be written as $\boldsymbol{E}_r \in \{\boldsymbol{E}_{r,1}, \boldsymbol{E}_{r,2}, \ldots, \boldsymbol{E}_{r,g}\}$ (where g is the number of selected non-metal types). According to Table 1, $\boldsymbol{E}_s \in \{\boldsymbol{E}_{\text{lead}}, \boldsymbol{E}_{\text{copper}}, \boldsymbol{E}_{\text{steel}}, \boldsymbol{E}_{\text{aluminum}}\}$ and $\boldsymbol{E}_r \in \{\boldsymbol{E}_{\text{epoxy resin}}, \boldsymbol{E}_{\text{hard rubber}}, \boldsymbol{E}_{\text{soft rubber}}, \boldsymbol{E}_{\text{organic glass}}\}$.

Table1 Mechanical properties of metamaterials

	Materials name	Acoustic velocity/($m \cdot s^{-1}$)	density / ($kg \cdot m^{-2}$)	Material before optimization	Material after optimization
Scatterer	Lead	2 160	11 600		
	Copper	4 726	8 960		Copper
	Steel	5 780	7 850	Steel	
	Aluminium	5 095	2 730		
Ligament and coating	Epoxy resin	2 680	1 180		
	Hard rubber	2 300	1 200	Epoxy resin	
	Soft rubber	300	1 300		Soft rubber
	Organic glass	1 180	2 680		
Matrix	Water	1 480	1 000	Water	Water

2.4 Optimization equation for bandgap

The geometric parameters and material type (elastic modulus of the material) of the acoustic metamaterial were defined as design variables in material selection optimization for acoustic metamaterial. Aiming to maximizing bandgap width and minimizing the lower-bound frequency, the bandgap optimization function for two-dimensional chiral acoustic metamaterial is established, as shows as follows:

$$
\begin{aligned}
\text{Find}: & \; r_0 = [r_{0,1}, r_{0,2}, \ldots, r_{0,i}]^{\mathrm{T}}, \quad i = 1,2,\ldots,I \\
& t_b = [t_{b,1}, t_{b,2}, \ldots, t_{b,m}]^{\mathrm{T}}, \quad m = 1,2,\ldots,M \\
& t_c = [t_{c,1}, t_{c,2}, \ldots, t_{c,n}]^{\mathrm{T}}, \quad n = 1,2,\ldots,N \\
& E_s = \{E_{s,1}, E_{s,2}, \ldots, E_{s,j}\}, \quad j = 1,2,\ldots,J \\
& E_r = \{E_{r,1}, E_{r,2}, \ldots, E_{r,g}\}, \quad g = 1,2,\ldots,G \\
\text{Max}: & \; \psi = w \cdot \xi + (1-w) \cdot \varsigma \\
\text{Subject to}: & \; (\Delta\omega_n)^* \geqslant (\Delta\omega_n)_0 \\
& \max: \omega_n(k)_0 \geqslant \max: \omega_n(k)^* \\
& G_{\text{total}} \leqslant G_{\text{total0}}
\end{aligned} \tag{5}
$$

where r_0 is the design variable of the radius of the i-dimensional scatterer; t_b is the design variable of the thickness of the m-dimensional ligament; t_c is the design variable of the thickness of the n-dimensional coating; $\boldsymbol{E}_s$ is the discrete-variable set of the elastic moduli of scatterer materials; $\boldsymbol{E}_r$ is the discrete-variable set of the elastic moduli of ligament and coating materials; G_{total0} and G_{total} are the cell mass in the initial design and optimized design, respectively, it satisfying $G_{\text{total}} \leqslant G_{\text{total0}}$.

3 Numerical calculation

3.1 Model description

Taking a two-dimensional tri-component hexa-chiral acoustic metamaterial for example, the numerically calculated the band structure of the solid-liquid acoustic metamaterial. The lattice constant is a=10 mm in initial design, and the other design parameters are as follows: r_0=1.5 mm, t_b= 0.6 mm, and t_c=0.6 mm. Both the ligaments and the coating are made from epoxy resin; the cylindrical scatterer is made from steel, and the matrices is

downloaded from www.ship-research.com

water. Table 1 lists the acoustic properties of the materials. The unit of material density is defined as kg/m^2 according to the two-dimensional problem, the cell mass of the acoustic metamaterial in the initial design is 0.008 8 kg.

The natural frequency and band structure of the cells of the acoustic metamaterial are calculated by using the finite-element software COMSOL Multiphysics 5.6. On this software, defining the design parameter, modeling geometric, finite-element division, material defining and periodic-boundary defining, are successively implemented.. The FEM of the hexa-chiral acoustic metamaterial is shown in Fig. 2.

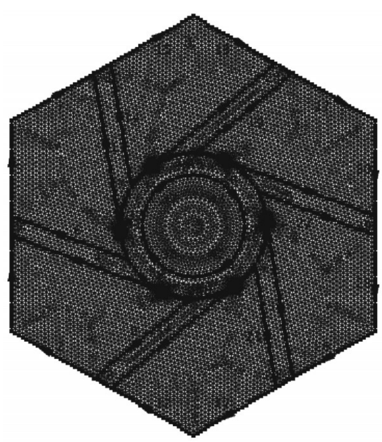

Fig. 2 Finite-element model of two-dimensional hexa-chiral acoustic metamaterial

3.2 Bandgap calculation

The wave vectors sweep the whole IBZ, and the sweep path is K → Γ → M → K. The linear dispersion relationship between wave vector and frequency can be obtained, the bandgap diagram of the hexa-chiral acoustic metamaterial is shown in Fig. 3. As shown in Fig. 3, there exist 10-band structure and 2 complete bandgap, the complete bandgap is shaded with gray.

The first bandgaps are located between the third and fourth bands structure, and the second bandgap is located between the ninth and tenth bands structure. In the present work, the parameter of the first bandgap is considered. The complete bandgap properties of the hexa-chiral acoustic metamaterial are shown in Table 2.

3.3 Bandgap optimization

In the bandgap optimization, the material properties (density, longitudinal wave velocities) and geometric parameters (scatterer diameter, ligaments thickness and coating thickness) are

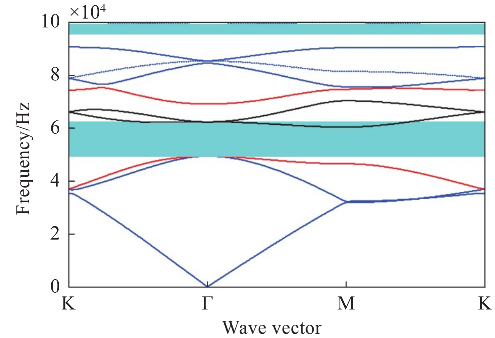

(a) Initial design

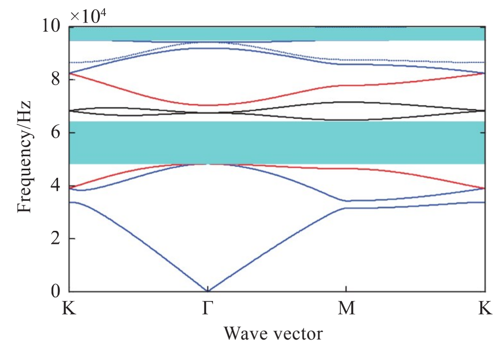

(b) Optimized design

Fig. 3 Band structure of hexa-chiral acoustic metamaterial

Table 2 Comparison of optimization results

Parameter	Initial design	Optimized design
Lower bound of frequency/Hz	49 362.5	48 314.2
Upper bound of frequency/Hz	62 277.1	64 815.4
Band-gaps width/Hz	12 914.6	16 501.2
Cell mass/kg	0.008 8	0.006 9
Normalization coefficient ψ	1.000 00	1.149 73

defined as design variables. The lead, copper, steel and aluminum are defined as candidate materials for scatterer, the material will be arbitrary lead, copper, steel and aluminum. The epoxy resin, hard rubber, soft rubber and Organic glass are defined as candidate materials for ligament and coating, the material will be arbitrary epoxy resin and silicon rubber. The acoustic properties of various materials are shown in Table 1. The ranges of the design variables were as follows: $r_0 \in (1.0\ \text{mm}, 2.0\ \text{mm})$, $t_b \in (0.3\ \text{mm}, 0.8\ \text{mm})$, and $t_c \in (0.5\ \text{mm}, 1.0\ \text{mm})$.

The material properties parameters (density, wave velocity) are discrete variable. Discontinuity in the properties of materials for the given materials' choice set, it makes material properties optimization is an inherent discrete optimization problem. On the other hand, the geometric parameters (scatterer diameter, ligaments or coating thickness) are continuous variable. Therefore, the bandgaps optimization problem is hybrid design variable problem. By defining the design variables, constraint condition and objectives function,

downloaded from www.ship-research.com

combination with Eq. 5, the bandgaps optimization is implemented by integrating the multidisciplinary optimization platform Isight. the bandgaps optimization is performed by the secondary development on the Isight integrated optimization platform, in which the genetic algorithm (GA) code is embedded.

After optimization, the band structure was obtained by bandgap optimization (Fig. 3(b)). The geometric parameters of the acoustic metamaterial are as follows: $r_0 = 1.29$ mm, $t_b = 0.42$ mm, and $t_c = 0.96$ mm. The cell materials change after the optimization, with the scatterer material changing into copper and the ligament and coating material changing into soft rubber. The width of the first bandgap increases by 3 586.6 Hz after the optimization, and its lower-bound frequency decreases by 1 048.3 Hz. The bandgap parameter coefficients are as follows: ξ = 1.277 6, ς = 1.021 7, and ψ=1.149 73; the cell mass of the acoustic metamaterial is 0.006 9 kg, as shown in Table 2.

4 Calculation of acoustic transmission loss

4.1 Model description

To verify the effect of bandgap optimization, the acoustic transmission of the acoustic metamaterial structure with finite length carried out. The acoustic metamaterial structure was composed of 10 layers of acoustic metamaterials arranged along the direction of wave propagation. An incident wave acted on the left side of the acoustic metamaterial structure, and the right side of the structure was an acoustic receiving zone. The left and right boundaries are defined as perfect matched layers to reduce the interference of reflective waves. Moreover, the periodic boundary condition is applied at the top and bottom edges. Fig. 4 shows the acoustic transmission model.

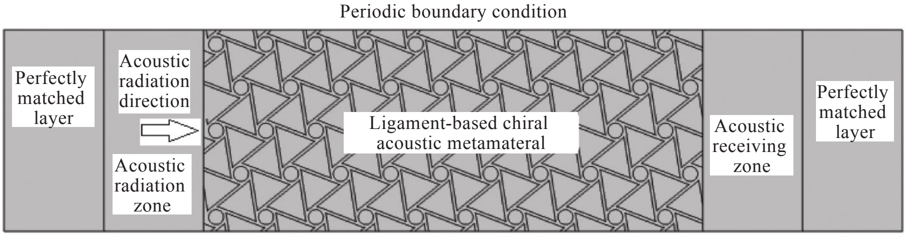

Fig. 4 Acoustic transmission model

4.2 Calculation of acoustic transmission

A plane wave of unit amplitude was incident on the acoustic metamaterial structure, and the integral values of the acoustic pressure on the left and right sides of the structure were defined as evaluation parameters. The numerically analysis the acoustic transmission loss of the ligament-based chiral acoustic metamaterial is implemented. The calculated frequencies ranged from 1 to 70 000 Hz, and the calculation step was 10 Hz, as shown in Fig. 5.

According to Fig. 5, the coefficient of acoustic transmission loss increases significantly within the frequency range of the bandgap. Moreover, the acoustic propagation and bandgap characteristics in different frequency ranges are consistent with expectations. The bandgap optimization reveals that the coefficient of acoustic transmission loss increases saliently within the bandgap and that the corresponding frequency bandwidth increases as well. The optimization effectively enhances the acoustic insulation capability of the acoustic metamaterial structure.

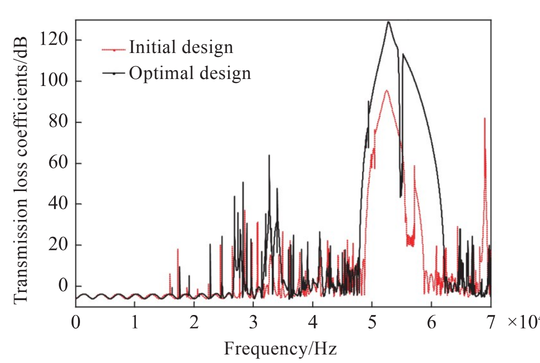

Fig. 5 Coefficient of acoustic transmission loss

The acoustic pressure fields at different frequencies are compared to evaluate the influence of the acoustic metamaterial structure for acoustic transmission, three frequency points were selected. The relative values of acoustic pressure fields are compared in Fig. 6, in which the left parts are field distributions from the initial design and the right ones are those from the optimized design.

In Fig. 6(a), the amplitudes of the acoustic

downloaded from www.ship-research.com

pressure at the output end before and after the optimization are both large when the acoustic wave frequency is within the passband of the acoustic metamaterial. Fig. 6(b) shows that the amplitudes of the acoustic pressure at the output end before and after the optimization are both small when the acoustic wave frequency is within the bandgap frequency. According to Fig 6(c), the acoustic wave frequency is within the passband in initial design, the amplitude of the acoustic pressure at the output end is very large; the acoustic wave frequency is within the bandgap after optimization, the amplitude of the acoustic pressure at the output end is small. The acoustic transmission loss coefficients in the frequency corresponding to bandgap frequency range increases significantly.

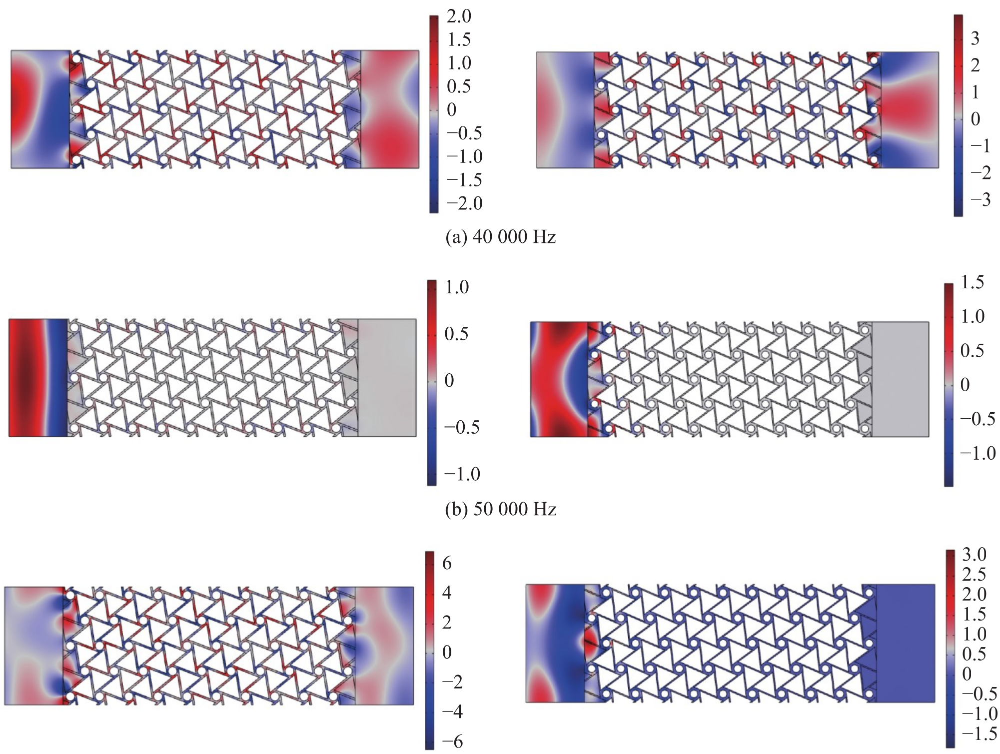

(a) 40 000 Hz

(b) 50 000 Hz

(c) 63 500 Hz

Fig. 6 Comparison of acoustic pressure field

5 Conclusions

Focusing on a ligament-based chiral acoustic metamaterial, the authors constructed an optimization equation considering mass for regulating the bandgap of the acoustic metamaterial. The main conclusions obtained by numerical calculation are as follows.

1) Compared with the initial design, the optimized design raises the bandgap width by 27.7% and lowers the lower-bound frequency of the bandgap by 1 048 Hz in the case of a mass reduction by 21.5%. and the results provide the idea of a lightweight design for hexa-chiral acoustic metamaterial .

2) Taking the mass of acoustic metamaterials into consideration in the optimization, it can provide technical support for the lightweight design of metamaterials.

3) The bandgap parameters can be normalized to transform the multi-objective optimization problem into a single-objective optimization problem, it improving optimization efficiency.

4) The chiral properties of acoustic metamaterials can provide more parameters for bandgap regulation.

References

[1] WU J H, MA F Y, ZHANG S W, et al. Application of acoustic metamaterials in low-frequency vibration and noise reduction [J]. Journal of Mechanical Engineering, 2016, 52(13): 68−78 (in Chinese).

[2] RUAN J Q, LU M H, CHEN Y F, et al. Metamaterial based on elastic mechanics [J]. Scientia Sinica Technologica, 2014, 44(12): 1261−1270 (in Chinese).

[3] TIAN Y, GE H, LU M H, et al. Research advances in acoustic metamaterials [J]. Acta Physica Sinica, 2019, 68(19): 194301 (in Chinese).

[4] XU W L, PENG W C, ZHANG J J, et al. Prospects of acoustic metamaterials for acoustic stealth [J]. Chinese Journal of Ship Research, 2020, 15(4): 19−27, 35 (in

downloaded from www.ship-research.com

Chinese).
[5] ZHANG Y N, CHEN K A, HAO X Y, et al. A review of underwater acoustic metamaterials [J]. Chinese Science Bulletin, 2020, 65(15): 1396−1410 (in Chinese).
[6] LIU Z Y, ZHANG X X, MAO Y W, et al. Locally resonant sonic materials [J]. Science, 2000, 289(5485): 1734−1736.
[7] BARAVELLI E, RUZZENE M. Internally resonating lattices for bandgap generation and low-frequency vibration control [J]. Journal of Sound and Vibration, 2013, 332(25): 6562−6579.
[8] SAXENA K K, DAS R, CALIUS E P. Three decades of auxetics research-materials with negative Poisson's ratio: a review [J]. Advanced Engineering Materials, 2016, 18(11): 1847−1870.
[9] ZHAI H F, XIANG H, MA X F, et al. Structural parameters optimization of a comb-like structure using locally resonant phononic crystals [J]. Modern Physics Letters B, 2019, 33(26): 1950312.
[10] SPADONI A, RUZZENE M, GONELLA S, et al.Phononic properties of hexagonal chiral lattices [J]. Wave Motion, 2009, 46(7): 435−450.
[11] EBRAHIMI H, MOUSANEZHAD D, NAYEB-HASHEMI H, et al. 3D cellular metamaterials with planar anti-chiral topology [J]. Materials & Design, 2018, 145: 226−231.
[12] HU L L, LUO Z R, YIN Q Y. Negative Poisson's ratio effect of re-entrant anti-trichiral honeycombs under large deformation [J]. Thin-Walled Structures, 2019, 141: 283−292.
[13] DUDEK K K. New type of rotation of chiral mechanical metamaterials [J]. Smart Materials and Structures, 2020, 29(11): 115027.
[14] XU W K, NING J Y, HAN S C, et al. Topological optimization design of two-dimensional solid/solid phonon crystals considering material parameters [J]. Journal of Shenyang Aerospace University, 2019, 36(5): 10−15 (in Chinese).
[15] XU W K, NING J Y, ZHANG M, et al. Three-phase microstructure topology optimization of two-dimensional phononic bandgap materials using genetic algorithms [J]. Acta Mechanica Solida Sinica, 2018, 31(6): 775−784.
[16] XIANG H, MA X F, XIANG J W. Optimization for a locally resonant phononic crystal of square spiral with circle inside [J]. IEEE Access, 2019, 17: 145988−145995.
[17] LI S B, CHEN T N, WANG X P, et al. Expansion of lower-frequency locally resonant band gaps using a double-sided stubbed composite phononic crystals plate with composite stubs [J]. Physics Letters A, 2016, 380(25/26): 2167−2172.
[18] HUANG Y, LIU S T, ZHAO J. A Gradient-based optimization method for the design of layered phononic band-gap materials [J]. Acta Mechanica Solida Sinica, 2016, 29(4): 429−443.

基于材料选型的手性声学超材料带隙优化分析

陈炉云*[1], 谢兴[2]
1 上海交通大学 海洋工程国家重点实验室,上海 200240
2 武汉第二船舶设计研究所,湖北 武汉 430205

摘　要:［**目的**］旨在寻求扩大带隙频率范围,降低带隙起始频率的方法,分析并优化声学超材料的带隙。［**方法**］分析几何参数与材料参数对声学超材料带隙特性的影响,提出最大化带隙宽度方法。通过归一化带隙参数系数,将多目标优化问题转化为单目标优化问题。基于材料选型优化理论实现组分材料的转换,建立基于轻量化的手性声学超材料带隙参数优化方程。以六韧带手性声学超材料为例,定义散射体、韧带及包覆物等结构设计参数和材料参数为设计变量,开展声学超材料的结构参数—材料选型的综合优化。［**结果**］优化结果显示,带隙宽度增加了27.7%,下界频率减少了1 048 Hz,初步达到了在声学超材料轻量化的基础上扩大带隙频率的目标;开展的有限长手性声学超材料结构的声传输分析验证了带隙优化方法的有效性。［**结论**］集成了结构参数—材料选型的综合优化可有效达到声学超材料轻量化的目标,研究成果可为新型声学超材料的设计提供技术参考。

关键词: 声学超材料; 材料选型; 带隙优化; 归一化; 声传输

downloaded from www.ship-research.com